# Phenothiazine-Modified Electrodes: A Useful Platform for Protein Adsorption Study

Bo-Hao Chiou, Yi-Ting Tsai, and Chong Mou Wang*

Department of Chemistry, National Taiwan Normal University, Taipei 116, Taiwan

S *Supporting Information*

ABSTRACT: Using glucose oxidase (GOx) as a target protein, we studied the adsorption of protein on the phenothiazine-modified electrodes and assessed the potential of using the electrodes in biochemical applications. Experiment results showed that thionine chloride (TC) and its structural analogues, such as toluidine blue and methylene blue, fluoresced under photochemical excitation after being immobilized on indium-doped tin oxide (ITO) electrodes fabricated using either diazotization-reduction or oxidative polymerization. The surface-bound phenothiazines exhibited substantial binding affinities to the protein. At a pH > 5, the adsorbate showed no sign of desorption even the electrodes were electrically biased with voltages between ±0.3 V vs SCE. Thus, emission decay occurred while GOx was injected over the electrodes, which was consistent with the observations made using conductive-mode atomic force microscopy (CM-AFM). Under a quiescent condition, the protein interacted with the immobilized TC via a pseudo-first-order kinetic mechanism. The reaction reached a maximum rate at a pH > 5, at which the rate constant was approximately 7×10^{-8} L/(U s). Under this condition, the adsorption rate increased as the level of the protein increased, regardless of pH, revealing application potential for GOx quantitation. The adsorption rate, however, decreased with a decrease in pH if the pH < 5. We concluded that static interactions played a crucial role. By monitoring $Fe(CN)_6^{3-/4-}$ taking place at the TC-modified electrodes in pH 7 solutions, we observed that the adsorption of GOx imposed impedance on $Fe(CN)_6^{3-/4-}$. The resulting charge-transfer resistance (R_{CT}) increased as the amount of the protein increased, leading to a conclusion that the protein could reach the maximum surface coverage when its concentrations were greater than 100 U/mL. The protein molecules were likely repel each other as approaching the TC sites. Despite this, they maintained the native bioactivity after being adsorbed, enabling the TC-modified electrodes to function as glucose sensors. Glucose concentrations between 1 and 60 mM could be detected. Long-term analysis, in addition, showed that the electrode responses to the analyte were consistent and reproducible. Phenothiazine-modified electrodes are evident as a useful tool for understanding the adsorption of protein on solid surfaces and quantifying proteins.
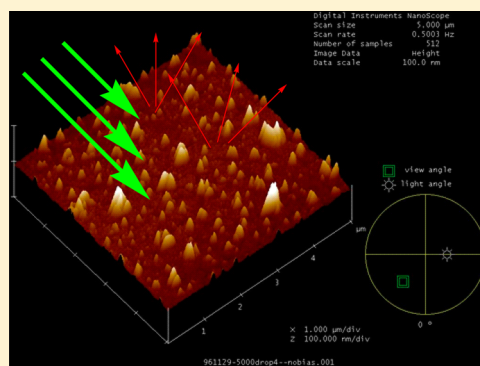
■ INTRODUCTION

Protein immobilization is essential to the integration of biochemical devices and their applications.[1] Various approaches for protein immobilization have been proposed and shown promise. The formation of covalent bonds prevents protein leakage, even in environments of high ionic strength[2] and physical adsorption,[3] including ionic adsorption,[4] specific adsorption,[5] and self-assembled monolayers,[6] enables the maintenance of the native structure and bioactivity of the immobilized protein, despite weak in adsorption affinity.

When proteins interact with surfaces, the photophysical or photochemical configurations of either side can be perturbed.[7,8] The resulting subtle distortions have become a driving force behind the recent technological advancements in biosensor devices, such as fluorescence-based protein probes.[9−14] These fluorescent probes exhibit high sensitivity and low noise. However, the reproducibility is still limited by dye aggregation,[15−17] which is also troubling dye-sensitized solar devices.[18] Recently, when we assessed the potential of using phenothia-

zine compounds in biochemical applications, we observed that thionine chloride (TC) and its structural analogues could be evenly attached to indium-doped tin oxide (ITO) conductive glass by using simple electrochemical modification processes, such as diazotization-reduction, oxidative polymerization, and atomic force microscope field-induced local oxidation (ALO), in which the immobilized phenothiazines showed the potential protein adhesive properties.[19,20] We also observed that some of the modified surfaces could fluoresce under photoexcitation, revealing the use of phenothiazines as potential fluorescent probes.

Quantitative and qualitative analytical techniques are vital to life sciences in many aspects, including the identification and quantitation of proteins. Optical methods are useful for these purposes. Diffuse-based spectroscopy,[21] for instance, is a

valuable supplement to standard histological techniques, showing promise for monitoring tumor oxygenation and metabolism[22] and performing tomography.[23] Considering the capacity of fiber optics for remote sensing[24] and the potential of phenothiazine for protein immobilization, we fabricated a fluorescent detection platform by using phenothiazine and fiber optics to study the protein adsorption kinetics and its potential for biochemical analysis. When glucose oxidase (GOx) was used as a target protein, we observed that the surfaces modified with phenothiazines exhibited emission decay. The decay rate increased exponentially with the protein concentration, revealing potential for protein quantitation. The protein maintained its native bioactivity after being adsorbed, endowing the TC-modified electrodes with sensitivity to glucose; glucose concentrations ranging from 1 to 60 mM could thus be detected in ambient conditions. Since the protein detection platform does not require elaborate preparation processes and the sensing mechanism is physical adsorption rather than covalent attachment, the device is regeneratable with acidic solutions (pH < 5). Hence, it is a potential alternative to the existing approaches for protein quantitation.

■ EXPERIMENTAL SECTION

Materials. Thionine chloride (TC), methylene blue (chloride salt, MB), and toluidine blue O (chloride salt, TB) were purchased from Aldrich. Glucose and glucose oxidase (GOx, E.C.1.1.3.4, from *Aspergillus niger*, 50 000 U/g) were supplied by Sigma. All the chemicals were used as received, without further purification. ITO glass squares (0.7 mm thick, 20 Ω/square; nominal coating thickness, 150−300 Å) were supplied by Delta Technologies. Before use, the ITO squares (0.5 × 0.5 cm^2) were thoroughly rinsed with 1 M sulfuric acid, chloroform, and deionized water to remove all the possible organic and inorganic contaminants, according to a procedure reported in the literature.[19] Buffer solutions with designated pHs (pH: 3−12; ionic strength = 0.1 M) were prepared from 0.1 M HCl with appropriate amount of KOH (0.1 M) to avoid anion effects on protein adsorption. The pH was monitored using a pH meter (Knick model 761).

Surface Modifications. For diazotization-reduction modification, TC and its structural analogues (1 mM) were dissolved in 0.1 M of HCl with equimolar NaNO$_2$. The solutions were then subjected to an immediate potential cycling between 0 and −0.6 V vs SCE at a constant scan rate (20 mV s^{-1}) in nitrogen, using the ITO squares as the working electrodes. For anodic polymerization, phenothiazine compounds (1 mM) were dissolved in 0.1 M of KCl instead. Electrochemical oxidation was carried out by sweeping the electrode potential from −0.5 to 1.2 V. Prior to morphological and photochemical characterizations, all the ITO squares (denoted as ITO|TC$_{DR}$, ITO|TB$_{DR}$, ITO|MB$_{DR}$, ITO|TC$_{AP}$, ITO|TB$_{AP}$, and ITO|MB$_{AP}$) were soaked in fresh KCl solutions (0.1 M) and cleaned with potential cycling (form 0.6 to −0.6 V vs SCE) to remove the unstable adsorbates (scan rate, 20 mV s^{-1}).

Apparatus. A potentiostat (PAR 283, EG&G) was used for cyclic voltammetry (CVs) and chronoamperometry. Unless otherwise specified, electrochemical experiments were conducted in a one-compartment cell equipped with a Pt counter electrode and an SCE reference electrode in nitrogen. Electrochemical impedance spectroscopic (EIS) analysis was performed on this potentiostat in conjunction with a lock-in amplifier (PAR 5210, EG&G) at pH 7 using Fe(CN)$_6^{3-}$ (1 mM) and equimolar Fe(CN)$_6^{4-}$ as redox probes. An ac perturbation (±5 mV, 0.1 MHz to 1 mHz) was superimposed with the formal potential of Fe(CN)$_6^{3-/4-}$. Data simulation was conducted using the electrochemical impedance software (Model 398, v. 1.26, EG&G). Emission analysis was performed using an Aminco-Bowman luminescence spectrophotometer (series 2) in conjunction with a Hamamatsu R2949 photomultiplier tube. For flow-injection analysis (FIA), a Watson Marlow (M 302S) microprocessor pump

drive/sample injection valve (20 μL loop) and a CC-5 electrochemical cell (BAS) were used. The stainless cover was replaced with the phenothiazine-modified ITO glass squares. The flow rate was 0.5 mL/min, and the sample volume was 20 μL unless otherwise mentioned. A Y-type optical fiber (Oriel M. 77404) was employed and set on the top of the ITO squares for light transmission and signal requisition. An atomic force microscope (AFM, Nanoscope III E, Digital Instrument Corp.) with a 10 μm scanner was used for surface imaging. The measurements were performed using a TiN-coated conductive tip (AIST/fpC10/TiN; spring constant: 0.1 N/m; width: 10 nm: contact mode). A home-built preamplifier, with a sensitivity of 1 nA/V and operational range from 1 pA to 10 nA, was used for current−voltage and conductive-mode AFM imaging measurements. This AFM was also employed to analyze the thickness of the phenothiazine films. Typically, three 1 μm^2 pits were shoveled for each sample using tips with a larger spring constant (Budget Sensors, Mode: Tap300AI, 20−75 N/m) to give the average data. Representative results are provided in Figure S1 (Supporting Information). Humidity was controlled using a home-built humidity controller.

■ RESULTS AND DISCUSSION

Figure 1 shows the diffuse fluorescence spectra of TC recorded after it was modified on conductive ITO glass as films via
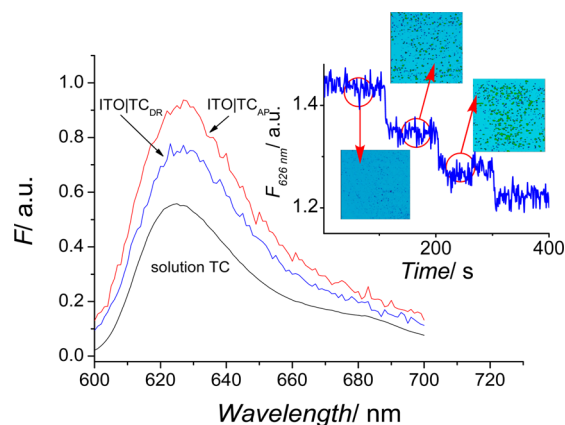

Figure 1. Emission spectra of TC (λ_{ex}: 570 nm) as dissolved in water (1 μM) and modified on ITO glass as films via anodic polymerization (ITO|TC$_{AP}$) and diazotization-reduction (ITO|TC$_{DR}$). Inset: systematic changes in the intensity of the 626 nm band and the surface morphology of an ITO|TC$_{AP}$ electrode with the number of injections of GOx (400 U/mL) after the electrode was integrated into a flow-injection system and injected over with the protein consecutively. AFM size: 1 × 1 μm^2. Scan rate: 1 Hz; bias: 0.5 V vs the grounded tip.

anodic polymerization and diazotization-reduction (denoted as ITO|TC$_{AP}$ and ITO|TC$_{DR}$, respectively). The spectra were similar in shape to the solution counterpart (1 μM in water), except that the peak wavelength shifted hypsochromically by 6 nm ($\lambda_{em,max}$: 626 nm). We attributed the red-shift to an enlarged structure and/or an increased stability resulting from polymerization and surface immobilization. In addition to the spectral difference, we noticed that the 626 nm band decreased systematically in intensity (denoted as F) as ITO|TC$_{AP}$ and ITO|TC$_{DR}$ were injected over with glucose oxidase (GOx) consecutively after the electrodes were integrated into a flow-injection system (Figure 1, inset). TC and its phenothiazine analogues had previously been identified as effective adhesives for proteins such as GOx.[20] The emission decay was thus ascribed to fluorescence blocking caused by adsorption of the protein. The AFM (conductive mode) images inset in Figure 1 supported this hypothesis. The protein molecules were

attracted to the TC sites on the electrodes, and their amount increased with the number of injections. The attraction strength was substantial. Electrochemical desorption[25] by biasing the electrodes with electric voltages varying between ±0.3 V could not remove the adsorbate to restore the normal intensity (Figure S2).

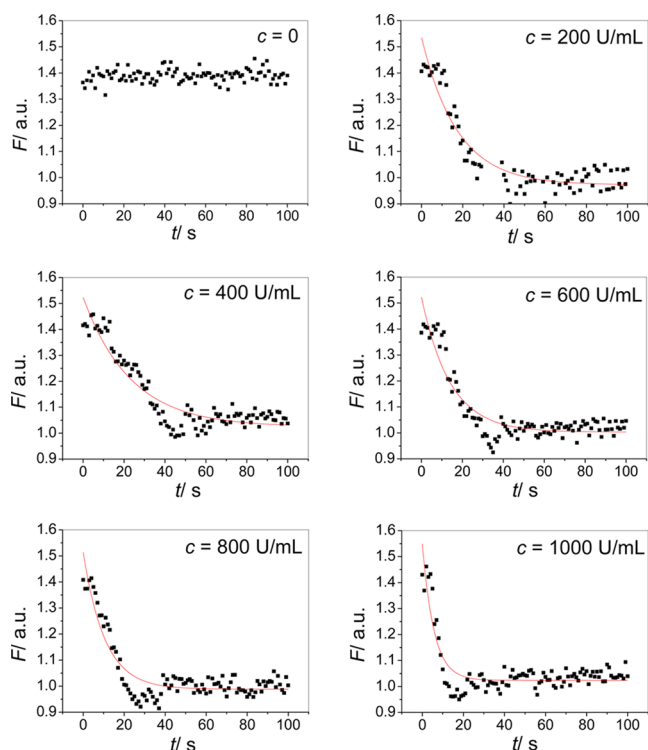Figure 2 shows that the emission intensity of ITO|TC$_{AP}$ decreased exponentially when GOx was present at a constant

Figure 2. Emission decay of ITO|TC$_{AP}$ (λ_{ex}: 570 nm; λ_{em}: 626 nm) caused by the adsorption of GOx (levels: 0–1000 U/mL; pH 7) under a quiescent condition.

level under a quiescent condition. The decay rate increased as the protein amount was increased, suggesting that the following reaction was involved:

$$\text{GOx}_{(aq)} + \text{TC}_{(im)} \rightleftharpoons \text{GOx@TC}_{(im)} \tag{1}$$
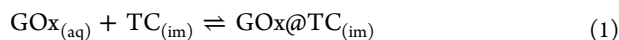
where TC$_{(im)}$ and GOx@TC$_{(im)}$ represent the TC sites and the protein adsorbed on the electrode, respectively. Following the rate law proposed in eq 2, we solved F as a function of time (t) and protein concentration (c) under the assumption that F was proportional to the number of TC site (n_{TC}):

$$dn_{TC}/dt = -\eta_1 n_{TC} c + \eta_2 (n_0 - n_{TC}) \tag{2}$$

$$
\begin{aligned}
F(t)/F(t=0) &= [\eta_1 c/(\eta_1 c + \eta_2)] \exp[-(\eta_1 c + \eta_2)t] \\
&\quad + [\eta_2/(\eta_1 c + \eta_2)]
\end{aligned}
\tag{3}
$$

Here, η_1 and η_2 represent the rate constants for the forward and backward processes, and n_0 represents the total number of the TC sites. According to eq 3, we expected the residual light, $F(t = \infty)$, to decrease with an increase in c:

$$F(t=0)/F(t=\infty) = 1 + (\eta_1/\eta_2)c \tag{4}$$

Simulation results based on eq 3 (red lines) fitted well with the experimental data. However, the resolved $F(t = \infty)$,

approximated by $F(t = 100 \text{ s})$, did not show a correlation with c. This inconsistency suggested that the protein could only be adsorbed on the outer surface of the modifier layer, in other words, $F(t = \infty)$ was mainly contributed by the inner TC sites. Considering this and the strong affinity of the TC sites to GOx, we hypothesized that $F(t = \infty)$ was a constant and $\eta_2 \ll \eta_1$. Equation 2 was therefore simplified into eq 5:

$$dn_{TC}/dt \approx -\eta n_{TC} c \tag{5}$$

The net intensity, i.e., $\Delta F(t) = F(t) - F(t = \infty)$, was expected to follow a simple exponential decay with c and $d[\ln\Delta F(t)]/dt$, or more precisely, $d\{\ln[\Delta F(t)/F(t = 0)]\}/dt$, to be a linear function of c.

$$\Delta F(t) = F(t=0) \exp(-\eta ct) \tag{6}$$

$$d\{\ln[\Delta F(t)/F(t=0)]\}/dt = -\eta c \tag{7}$$

By approximating $F(t = \infty)$ with $F(t = 100 \text{ s})$, we calculated $d\{\ln[\Delta F(t)/F(t = 0)]\}/dt$ for $c > 200$ U/mL based on eq 7; the results are plotted against c and shown in Figure 3. Despite
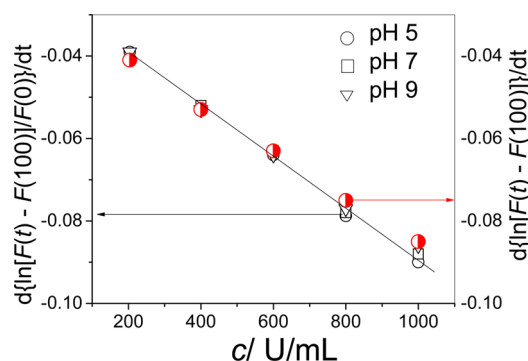

Figure 3. Dependence of the adsorption rate of GOx on ITO|TC$_{AP}$, expressed as $d\{\ln[F(t) - F(100)]\}/F(0)\}dt$ vs c (200–1000 U/mL), at pHs of 5, 7, and 9. The data of pH 7 are replotted as $d\{\ln[F(t) - F(100)]\}/dt$ vs c (red broken circle) for comparison.

deviations appearing near the region of high c values, $d\{\ln[\Delta F(t)/F(t = 0)]\}/dt$ showed a linear correlation with c, which held for a wide range in pH between 5 and 9. The discrepancies were ascribed to the disregard of the backward process and nonideal single-layer adsorption. Electrode-surface fouling, e.g., fluctuations in film thickness, could also cause similar problems. For this possibility, we carried out the control experiments in the absence of the protein, which showed that the $F(t = 0)$ of ITO|TC$_{AP}$ could be regarded as a constant when the TC film was thicker than 3 nm; representative results are shown in Figure 4. We examined ITO|TC$_{DR}$ for verification. Similar conclusions were drawn, as was true for the films of TB and MB. Based on the model proposed in Figure S3 under the assumptions that the phenothiazine film was composed of an infinite number of laminates (width = dx) and the fluorophores in each laminate emitted fluorescence with equal intensity (f_o) after being photoexcited, $F(t)$ was formulated as

$$F(t=0) = \int_0^A dS \int_0^d dx(f_x c^*) \tag{8}$$

where d is the film thickness, dS is the cross section, A is the area of the optical fiber, c^* is the hypothetical concentration of the fluorophore in the film, and f_x is the intensity of the fluorescence emitted from the adsorption site located at a
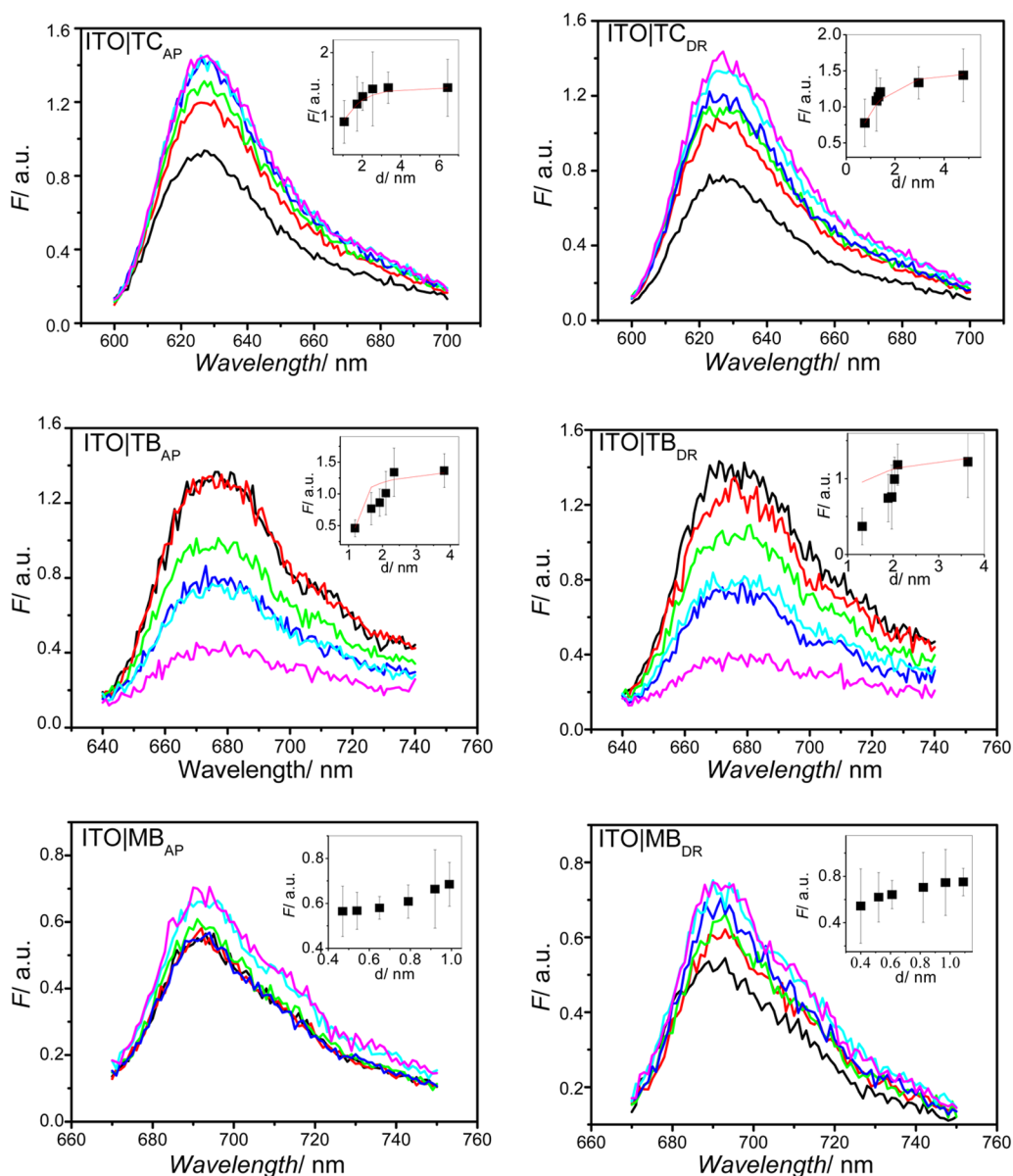
Figure 4. Diffuse fluorescence spectra of TC, TB, and MB films with various thickness prepared via anodic polymerization (AP) and diazotization-reduction (DR) processes. Inset: correlation between peak intensity (F) and film thickness (d).

distance x from the surface, collected at $x = 0$. Provided that f_0 decreased as x increased because of internal absorption, f_x was related to f_0 as

$$f_x = f_0 \exp(-\kappa x) \tag{9}$$

where κ is the extinction coefficient. $F(t = 0)$ was shown to be independent of d as $d \to \infty$.

$$F(t = 0) = (f_0 c^* A/\kappa)[1 - \exp(-\kappa d)] \tag{10}$$

On the basis of eq 10, we estimated κ for TC and TB; the value was determined to be approximately 1 nm^{-1}. Simulation results (red lines) based on this result fitted well with the experimental data. The value of $F(t = 0)$ for $d = 3\kappa^{-1}$ assumed 96% of the maximum ($f_0 c^* A/\kappa$). This explained why the emission of the TC-modified electrodes tended to be a constant when the TC film was thicker than 3 nm. We accordingly proposed that once $d \gg 3\kappa^{-1}$, fluctuations in thickness or uniformity would not pose problems for the phenothiazine-modified electrodes.

Equation 7 was thus simplified into eq 11 to explain the similarity of $d[\ln \Delta F(t)]/dt_{t=0}$ (approximated by $d\{\ln[F(t) - F(100\ \text{s})]/d\}t_{t=0}$) to $d\{\ln[\Delta F(t)/F(t = 0)]\}/dt$ as plotted against c (red broken circles in Figure 3).

$$d[\ln \Delta F(t)]/dt \approx -\eta c \tag{11}$$

From the analytical point of view, eq 11 is more practical than eq 7 for applications. Attempts were also made to estimate κ for MB. The results were unproductive because of the difficulty in growing films thicker than 1 nm. This problem was attributed to a lack of primary amine. Primary amine groups are essential to aromatic compounds when they undergo anodic polymerization and diazotization-reduction processes. MB may thus result in an $F(t = 0)$ much smaller than those of the other two analogues.

In addition to the film-thickness dependency, we also investigated other factors that might interfere with the TC-modified electrodes in protein quantitation. EIS analysis showed that the electron exchange between $Fe(CN)_6^{3-}$ and

$Fe(CN)_6^{4-}$ occurring at $ITO|TC_{DR}$ ($d > 3$ nm, pH 7) became more sluggish when GOx was incorporated with elevated levels; the associated complex plots are shown in Figure 5A. On the
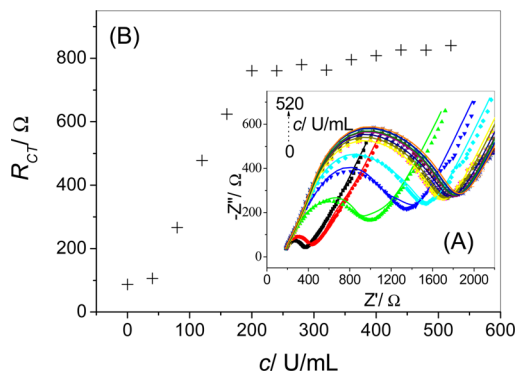

Figure 5. (A) EIS spectra of $ITO|TC_{DR}$ recorded in pH 7 solutions containing $Fe(CN)_6^{3-}$ and $Fe(CN)_6^{4-}$ (1 mM each) added with GOx of 0, 40, 80, 120, 160, 200, 240, 280, 320, 360, 400, 440, 480, and 520 U/mL. The solid lines are the simulation results. (B) Plot of R_{CT} vs c.

basis of a simple Randles circuit (Figure S4), we analyzed the associated charge-transfer resistance (R_{CT}). The resolved R_{CT} increased rapidly with c up to 100 U/mL and tended to a saturation value ($R_{CT,s}$) as c exceeded 100 U/mL (Figure 5B). The variation in R_{CT} confirmed that the TC_{DR} film was as attractive to GOx as the TC_{AP} film was and, in addition, suggested that the protein was likely to obtain a maximum surface coverage when c approached 100 U/mL. By defining surface coverage (θ) as $R_{CT}/R_{CT,s}$, we calculated $\ln\{c/[\theta/(1 - \theta)]\}$ for each c based on the Frumkin isotherm expressed in eq 12;[26] the results in terms of $\ln\{c/[\theta/(1 - \theta)]\}$ vs θ are shown in Figure 6.

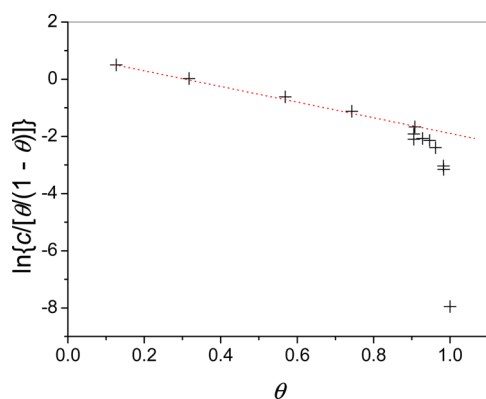$$\ln\{\beta c/[\theta/(1 - \theta)]\} = g\theta \tag{12}$$

Figure 6. Surface coverage analysis for the adsorption of GOx on $ITO|TC_{DR}$ at pH 7, expressed as $\ln\{c/[\theta/(1 - \theta)]\}$ vs θ (data in Figure 5).

Here, β represents for the equilibrium constant for reaction 1, and the parameter g represents the way in which increased coverage changes the adsorption energy of the adsorbate. The g factor was estimated to be −1 J/mol per mol/cm^2, suggesting that the protein molecules might repel each other during adsorption, which is consistent with the negatively charged structure of the protein at a pH of 7 predicted according to its

pI value ($\sim$4.3).[27] That repulsive interaction provided another explanation for the deviations shown in Figure 3.

We also studied the effect of pH on reaction 1. In the absence of protein, FIA analysis showed that increasing pH enhanced the emission intensity of $ITO|TC_{AP}$ ($d > 3$ nm, Figure 7). The results were considerably reproducible. We thus
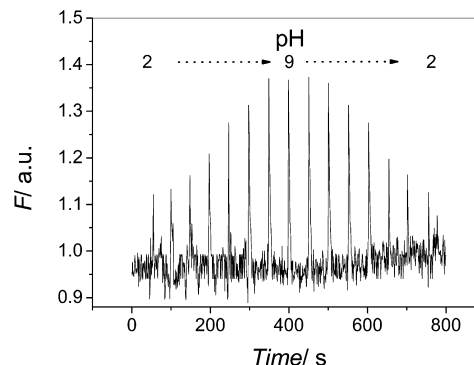

Figure 7. FIA analysis for the effect of pH on the emission of $ITO|TC_{AP}$. Buffer solutions of pH 2−9 were injected over the electrode with an HCl eluent (0.1 M).

concluded that the TC film prepared via anodic polymerization was robust. The intensity, however, dropped rapidly when GOx was incorporated, and the decay rate was a function of pH (Figure 8). Here, the experiments were carried out under a
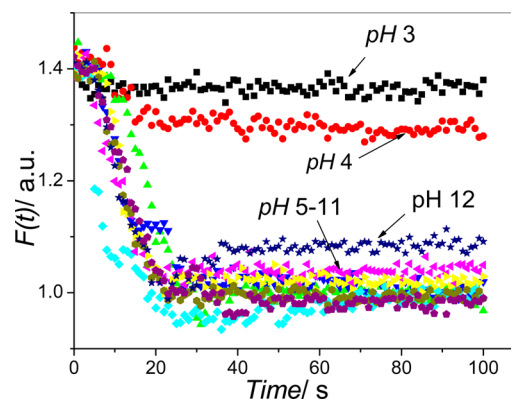

Figure 8. Changes in the emission intensity of $ITO|TC_{AP}$ upon adding 400 U/mL of GOx at pH: 3−12 under a quiescent condition.

quiescent condition. The contrast between these results highlighted that TC was an effective protein binder, and reaction 1 was pH-sensitive. Accordingly, we disregarded the effect of pH on the TC film and calculated η for reaction 1 at each pH. Based on eq 11, the maximum value was estimated to be 6.5×10^{-8} L/(U s), approximately 100 times that obtained at a pH of 3. The results in terms of $\eta/\eta_{pH\ 3}$ are shown in Figure 9, in which the adsorption of GOx increased in speed with pH from 3 to 5 and reached the plateau at a pH > 5. The residual light also indicated pH dependence. Approximated by $F(t = 100$ s), $F(\infty)$ showed a trend opposite to that of η (inset of Figure 9). This result provided a clue for the surface coverage of GOx on the TC-modified electrodes. We previously postulated that $F(\infty)$ was mainly contributed by the sites in the inner layers of the TC film. It is obvious that the hypothesis is correct only if the outer layer is fully covered by the protein. Since the unoccupied sites on the outer layer can
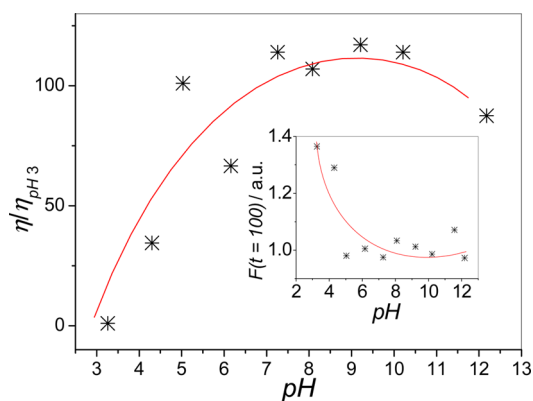
Figure 9. Analysis for the adsorption of GOx on ITO|TC$_{AP}$, expressed as the relative rate constant $(\eta/\eta_{pH\,3})$ vs pH. Inset: relationship between $F(\infty)$ (approximated by $F(t = 100\ s)$) and pH.

contribute as well, $F(\infty)$ turns out to be a useful measure of the number of the unoccupied sites or the surface coverage of the protein. According to the inset in Figure 9, the protein obtained the greatest surface coverage at a pH > 5. An environment too acidic (pH < 5) or too basic (pH > 12) was unfavorable for reaction 1. For the low θ in acidic solutions, static repulsion is likely the cause because the protein and the adsorption site are all positively charged, as indicated by the pI value of GOx, the pK_a of the protonated amine groups on TC (~5), and the structure of thionine. For the results observed at pH 12, protein denaturation is likely. Despite these, η and θ remained almost constant for 5 < pH < 10. The TC-modified electrodes are thus applicable to protein analysis in ambient conditions, without the need of specific buffers, which explains why a variation in pH from 5 to 9 did not cause interference to the linear correlations shown in Figure 3. It is also worthwhile to note that the adsorbed protein molecules still maintained the native bioactivity; the TC-modified electrodes (denoted as ITO|TC$_{AP}$|GOx) could thus function as glucose sensors. Figure 10 shows
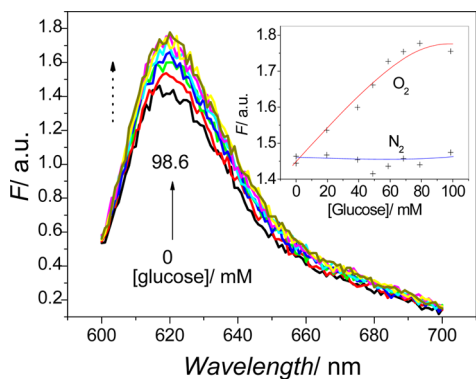

Figure 10. Diffuse fluorescence spectra of ITO|TC$_{AP}$|GOx recorded in aerated solutions with glucose at 0, 19.6, 39.2, 49.0, 58.8, 68.6, 79.0, and 98.6 mM without specific pH buffer. Inset: relationships between peak intensity and [glucose] in nitrogen and oxygen, respectively.

that when ITO|TC$_{AP}$|GOx was brought into contact with glucose in aerated solutions without pH buffers, its emission increased in intensity as the amount of the analyte increased, leading to a linear correlation ranging from 1 to 60 mM. For the glucose sensitivity, control experiments showed that the emission intensity was a function of O_2, H_2O_2, and pH. At a pH of 7, excluding O_2 could not produce similar results (inset in

Figure 10). Substituting glucose with hydrogen peroxide revealed a bleaching effect instead (Figure S5). Since oxygen exhibited an effect similar to H_2O_2 in the absence of glucose, the glucose sensitivity was tentatively ascribed to local proton depletion resulting from the transduction of glucose and generation of H_2O_2 by GOx and O_2 on the TC film. In addition to the sensitivity, FIA analysis of the electrode over a wide range of concentration of GOx showed that the electrode responses were substantially reproducible after the electrode was resting in pH 7 buffer solutions for 24 h (Figure S6). These results supported that TC layer was durable and its attraction affinity to GOx was significant.

■ CONCLUSION

Using GOx and diffuse fluorescence spectroscopic techniques, we demonstrated that phenothiazine compounds such as TC and its structural analogues are useful for studying the adsorption kinetics of proteins. TC is a fluorescent protein binder. Although it does not form covalent links with proteins, it can attract proteins through static interactions after being immobilized on ITO glass via simple electrochemical modification processes. These properties lead to protein adsorption and emission decay. The protein can therefore be detected and quantified. By manipulating pH and using $Fe(CN)_6^{3-/4-}$ as redox probes, we conclude that the adsorption of GOx can reach the highest rate at a pH > 5. In this case, the rate shows an exponential correlation with the protein level, regardless of pH. When the protein level is higher than 100 U/mL, GOx is able to form the greatest surface coverage. The protein molecules maintain their native bioactivity after being adsorbed on the TC films and endow the surfaces with sensitivity to glucose. The responses to glucose are significant and considerably reproducible. Because the electrodes do not require elaborate preparation processes and the protein-sensing mechanism only involves physical adsorption, the phenothiazine-modified electrodes are a potential alternative to the existing techniques for protein analysis.

■ ASSOCIATED CONTENT

ⓢ Supporting Information
Experimental details for the determination of the thickness of phenothiazine films and the chronoamperograms for the electrochemical desorption of GOx; a model accounting for the relationship between the emission intensity of phenothiazine films and their thickness, an equivalence circuit for the charge-transfer reaction of $Fe(CN)_6^{3-/4-}$ taking place at the TC-modified electrodes, the effect of H_2O_2 on the TC-modified electrodes, and a long-term FIA analysis of the electrode response to glucose. This material is available free of charge via the Internet at http://pubs.acs.org.

■ AUTHOR INFORMATION

Corresponding Author
*E-mail checcmw@ntnu.edu.tw (C.M.W.).

Notes
The authors declare no competing financial interest.

■ ACKNOWLEDGMENTS

■ REFERENCES

(1) Thevenot, P.; Hu, W.; Tang, L. Surface Chemistry Influences Implant Biocompatibility. *Curr. Top. Med. Chem.* **2008**, *8*, 270−280.

(2) Endrizzi, B. J.; Huang, G.; Kiser, P. F.; Stewart, R. J. Specific Covalent Immobilization of Proteins through Dityrosine Cross-links. *Langmuir* **2006**, *22*, 11305−11310.

(3) Rusmini, F.; Zhong, Z.; Feijen, J. Protein Immobilization Strategies for Protein Biochips. *J. Biomacromol.* **2007**, *8*, 1775−1789.

(4) Mateo, C.; Abian, O.; Fernandez-Lafuente, R.; Guisan, J. M. Reversible Enzyme Immobilization via a Very Strong and Non-distorting Ionic Adsorption on Support-Polyethylenimine Composites. *Biotechnol. Bioeng.* **2000**, *68*, 98−105.

(5) Nakanishi, K.; Sakiyama, T.; Kumada, Y.; Imamura, K.; Imanaka, H. Recent Advances in Controlled Immobilization of Proteins onto the Surface of the Solid Substrate and Its Possible Application to Proteomics. *Curr. Proteomics* **2008**, *5*, 161−175.

(6) Hodneland, C. D.; Lee, Y.-S.; Min, D.-H.; Mrksich, M. Selective Immobilization of Protein to Self-Assembled Monolayers Presenting Active Site Directed Capture Ligands. *Proc. Natl. Acad. Sci. U. S. A.* **2002**, *99*, 5048−5052.

(7) Lu, J. R.; Su, T. J.; Thomas, R. K. Binding of Surfactants onto Preadsorbed Layers of Bovine Serum Albumin at the Silica-Water Interface. *J. Phys. Chem. B* **1998**, *102*, 10307−10315.

(8) Gray, J. J. The Interaction of Proteins with Solid Surfaces. *Curr. Opin. Struct. Biol.* **2004**, *14*, 110−115.

(9) Cao, S.-H.; Xie, T.-T.; Cai, W.-P.; Liu, Q.; Li, Y.-Q. Electric Field Assisted Surface Plasmon-Coupled Directional Emission: An Active Strategy on Enhancing Sensitivity for DNA Sensing and Efficient Discrimination of Single Base Mutation. *J. Am. Chem. Soc.* **2011**, *133*, 1787−1789.

(10) Suzuki, Y.; Yokoyama, K. Design and Synthesis of Intra-molecular Charge Transfer-Based Fluorescent Reagents for the Highly-Sensitive Detection of Proteins. *J. Am. Chem. Soc.* **2005**, *127*, 17799−17802.

(11) Wang, F.; Wen, J.; Huang, L.; Huanga, J.; Ouyang, J. A highly Sensitive "Switch-on" Fluorescent Probe for Protein Quantification and Visualization Based on Aggregation-induced Emission. *Chem. Commun.* **2012**, *48*, 7395−7397.

(12) Hoefelschweiger, B. K.; Duerkop, A.; Wolfbeis, O. S. Novel Type of General Protein Assay Using a Chromogenic and Fluorogenic Amine-Reactive Probe. *Anal. Biochem.* **2005**, *344*, 122−129.

(13) Royer, C. A. Probing Protein Folding and Conformational Transitions with Fluorescence. *Chem. Rev.* **2006**, *106*, 1769−1784.

(14) Gerasimova, Y. V.; Peck, S.; Kolpashchikov, D. M. Enzyme-Assisted Binary Probe for Sensitive Detection of RNA and DNA. *Chem. Commun.* **2010**, *46*, 8761−8763.

(15) Murphy, J. N.; Cheng, A. K. H.; Yu, H.-Z.; Bizzotto, D. On the nature of DNA Self-Assembled Monolayers on Au: Measuring Surface Heterogeneity with Electrochemical In Situ Fluorescence Microscopy. *J. Am. Chem. Soc.* **2009**, *131*, 4042−4050.

(16) Pasternack, R. F.; Fleming, C.; Herring, S.; Collings, P. J.; DePaula, J.; DeCastro, G.; Gibbs, E. J. Aggregation Kinetics of Extended Porphyrin and Cyanine Dye Assemblies. *Biophys. J.* **2000**, *79*, 550−560.

(17) Bagwe, R. P.; Hilliard, L. R.; Tan, W. Surface Modification of Silica Nanoparticles to Reduce Aggregation and Nonspecific Binding. *Langmuir* **2006**, *22*, 4357−4362.

(18) Nepomnyashchii, A. B.; Parkinson, B. A. Influence of the Aggregation of A Carbazole Thiophene Cyanoacrylate Sensitizer on Sensitized Photocurrents on ZnO Single Crystals. *Langmuir* **2013**, *29*, 9362−9368.

(19) Wu, S.-W.; Huang, H. Y.; Guo, Y. C.; Wang, C. M. ALO-Patternable Artificial Flavin: Phenazine, Phenothiazine and Phenox-azine. *J. Phys. Chem. C* **2008**, *112*, 9370−9376.

(20) Huang, H. Y.; Wang, C. M. Phenothiazine: An Effective Molecular Adhesive for Protein Immobilization. *J. Phys. Chem. C* **2010**, *114*, 3560−3567.

(21) Zonios, G.; Perelman, L. T.; Backman, V.; Manoharan, R.; Fitzmaurice, M.; Van Dam, J.; Feld, M. S. Diffuse Reflectance Spectroscopy of Human Adenomatous Colon Polyps In Vivo. *Appl. Opt.* **1999**, *38*, 6628−6637.

(22) Palmer, G. M.; Viola, R. J.; Schroeder, T.; Yarmolenko, P. S.; Dewhirst, M. W.; Ramanujam, N. Quantitative Diffuse Reflectance and Fluorescence Spectroscopy: A Tool to Monitor Tumor Physiology In Vivo. *J. Biomed. Opt.* **2009**, *14*, 024010.

(23) Milstein, A. B.; Oh, S.; Webb, K. J.; Bouman, C. A.; Zhang, Q.; Boas, D. A.; Millane, R. P. Fluorescence Optical Diffusion Tomography. *Appl. Opt.* **2003**, *42*, 3081−3094.

(24) Lee, B. Review of the Present Status of Optical Fiber Sensors. *Opt. Fiber Technol.* **2003**, *9*, 57−79.

(25) Arinaga, K.; Rant, U.; Knežević, J.; Pringsheim, E.; Tornow, M.; Fujita, S.; Abstreiter, G.; Yokoyama, N. Controlling the Surface Density of DNA on Gold by Electrically Induced Desorption. *Biosens. Bioelectron.* **2007**, *3*, 326−331.

(26) Bard, A. J.; Faulkner, L. R. *Electrochemical Methods, Fundamentals and Applications*; Wiley: New York, 1980; pp 516−518.

(27) Kim, K. K.; Fravel, D. R.; Papavizas, G. C. Glucose Oxidase As the Antifungal Principle of Talaron from Talaromyces Flavus. *Can. J. Microbiol.* **1993**, *36*, 760−764.